Journal of Crystal Growth 312 (2010) 3276–3281

Contents lists available at ScienceDirect

Journal of Crystal Growth

journal homepage: www.elsevier.com/locate/jcrysgro

Optical and electrical properties of lithium doped nickel oxide films deposited by spray pyrolysis onto alumina substrates

I.A. Garduño [a], J.C. Alonso [a,*], M. Bizarro [a], R. Ortega [b], L. Rodríguez-Fernández [c], A. Ortiz [a]

[a] Instituto de Investigaciones en Materiales, Universidad Nacional Autónoma de México. A. P. 70-360, Coyoacán 04510, D.F., México
[b] Facultad de Ciencias, Universidad Nacional Autónoma de México. A. P. 70-542, Coyoacán 04510, D.F., México
[c] Instituto de Física, Universidad Nacional Autónoma de México. A. P. 20-364, Coyoacán 01000, D.F., México

ARTICLE INFO

Article history:
Received 30 April 2010
Received in revised form
12 August 2010
Accepted 16 August 2010
Communicated by D.P. Norton
Available online 21 August 2010

Keywords:
A1. Characterization
A3. Spray pyrolysis
B1. Metal oxides
B2. Semiconducting materials

ABSTRACT

Non-doped and lithium doped nickel oxide crystalline films have been prepared onto quartz and crystalline alumina substrates at high substrate temperature (600 °C) by the pneumatic spray pyrolysis process using nickel and lithium acetates as source materials. The structure of all the deposited films was the crystalline cubic phase related to NiO, although this crystalline structure was a little bit stressed for the films with higher lithium concentration. The grain size had values between 60 and 70 nm, almost independently of doping concentration. The non-doped and lithium doped films have an energy band gap of the order of 3.6 eV. Hot point probe results show that all deposited films have a p-type semiconductor behavior. From current–voltage measurements it was observed that the electrical resistivity decreases as the lithium concentration increases, indicating that the doping action of lithium is carried out. The electrical resistivity changed from 10^6 Ω cm for the non-doped films up to 10^2 Ω cm for the films prepared with the highest doping concentration.

1. Introduction

Nickel oxide (NiO) is a transition metal oxide p-type semiconductor that crystallizes in a rock salt structure and has a wide energy band gap in the range from 3.6 to 4.0 eV. Due to its physical properties, it has a wide range of applications, such as: transparent conducting contact, electro-chromic display devices, lasers, smart windows, luminescent materials, solid electrolytes, fuel cell electrodes and, in particular, as the active material in chemical sensors [1–4].

For chemical gas sensor applications the films are required to be deposited onto relatively inert substrates and to have a good electrical conductivity. To fulfill the former need is that alumina sheets are commonly used as substrates in the preparation of chemical gas sensors whose response is based on changes in the electrical conductivity of the active layer. On the other hand, given that gas sensors use the change in electrical resistance due to the action of the gas of interest as a response, the control of the magnitude of this parameter is important. Although stoichiometric NiO is an electrical insulator, its resistivity can be tailored to fulfill the above requirement by the creation of nickel vacancies, which results in increase in the amount of Ni^{3+} ions, or by the addition of monovalent atoms like lithium or interstitial oxygen in NiO crystallites [5]. Thin films of this material have been applied as an active layer in chemical gas sensor devices to detect hydrogen, carbon monoxide, nitrous oxide and formaldehyde [6–8], showing good response characteristics.

NiO thin films have been prepared by physical and chemical deposition techniques, such as: DC reactive sputtering and RF magnetron sputtering, soft chemical routes, chemical vapor deposition, photochemical deposition and spray pyrolysis [9–13]. Among those deposition techniques, the spray pyrolysis is the cheapest and the easiest technique for thin film deposition. In general, high quality metallic oxides thin films have been produced by this technique in large areas for different applications. There are some reports on the deposition of nickel oxide thin films by the spray pyrolysis process using nickel chloride, nickel acetylacetonate and nickel acetate as nickel source materials [14–16], all of them report the films' deposition at relatively low temperatures (300–500 °C). In some of those reports the thin film deposition was carried out in a pulsed spray way.

On the other hand, the detection process of gases in resistive chemical gas sensors is a surface phenomenon, which consists in the des-adsorption of gases after a chemical reaction with the gas of interest, present in the surrounding atmosphere, with the modification of the electrical resistance of the device. It has been observed that textured oxides films are suitable materials for applications in the preparation of resistive chemical gas sensors. In general, the surface areas of grain boundary per unit of mass in

* Corresponding author.
E-mail address: alonso@servidor.unam.mx (J.C. Alonso).

0022-0248/$ - see front matter © 2010 Elsevier B.V. All rights reserved.
doi:10.1016/j.jcrysgro.2010.08.020

textured thin films are larger than those of continuous ones; this fact results in a greater sensitivity of devices [17]. Suitable values of deposition parameters must be determined to deposit textured metallic oxide thin films by the spray pyrolysis technique.

In this work we report the deposition of nickel oxide films by spray pyrolysis onto alumina substrates, at high substrate temperatures using nickel acetate (NiAc) and lithium acetate (LiAc) as nickel and lithium source materials, respectively, in a mixed water–alcohol spray solution. We also studied the effect of lithium doping on the crystalline structure of the films and on the optical and electrical properties.

2. Experimental

The source materials used were nickel(II) acetate tetra-hydrate, 98% (NiAc) and lithium acetate di-hydrate, 98% (LiAc) from Aldrich. For doping, LiAc was added to the starting solution. Previous to depositing the NiO films, the substrates were cleaned with trichloroethylene, methanol and acetone, in an ultrasonic bath, and dried with a flow of nitrogen gas. In order to measure the thickness of the deposited films, a small area of a surface of the substrates was covered with cover glass to form a step during film deposition, and to improve heat transfer between the tin thermal bath and the substrate itself, a graphite layer was painted on the surface of the substrate in contact with the tin bath. Also, TGA test was performed on Ni(Ac), where it was found that temperatures above 350 °C are needed to decompose it. Since most of the NiO films made by spray pyrolysis had been grown on glass substrates [18], initially, some films were deposited onto pyrex glass sheets in order to establish a set of suitable deposition conditions. In this case for the nickel oxide deposition we used a 0.025 M start solution of Ni(Ac) dissolved in a mixture of three parts of methanol anhydrous and one part of deionized water, and the solution and air flow rates were set at 7 cm^3/min and 10 L/min, respectively. The nozzle–substrate distance was 30 cm and the deposition time was 20 min. The substrate temperatures were 360, 380, 400, 420 and 440 °C. The samples grown at 360 and 380 °C were darkish, which means that the starting solution was not completely decomposed, with the probable incorporation of carbon in deposited material. Meanwhile the films grown at higher temperatures looked transparent, meaning that there were no residuals of the organic radicals incorporated in the samples. The thickness of the grown films shows a decaying behavior as the substrate temperature is increased, which is a typical behavior in spray pyrolysis deposited films. In order to determine the optical band gap and due to a possible application as the active layer in gas sensors, clear fused quartz and alumina sheets were used as substrates. The substrate temperature chosen for film deposition on these substrates was 400 °C. However, using the previously established deposition parameters there was no film deposition on both types of substrates. Due to this, it was necessary to find new deposition parameters to deposit NiO films onto the fused quartz and alumina substrates. The conditions under which we obtained film deposition were the following. The NiAc solution was increased to 0.05 M; the nozzle–substrate distance was diminished to 15 cm; the gas flow rate was set at 8 L/min; the solution flow rate and deposition time were kept constants at 7 cm^3/min and 20 min, respectively. The substrate temperatures were 500, 550, 600 and 650 °C. In this case the samples deposited at 500 and 550 °C looked darkish and their adhesion to substrates was poor. Samples grown at 600 and 650 °C were transparent (observed on quartz substrates) and were well adhered to both kinds of substrates. This time the substrate temperature of 600 °C was chosen for further samples. Under the latter conditions lithium doping of NiO films was carried out adding LiAc to the start solution. The relative LiAc concentration was varied from 0 to 50 at% at steps of 5 at%.

The crystalline structure of all the deposited films was determined by X-ray diffraction measurements using a SIEMENS D500, with Cukα wavelength (1.5406 Å) and an incidence angle of 1°. The obtained X-ray diffraction spectra were interpreted in reference to the PDF cards: 00-047-1049 for NiO and 00-046-1212 for Al2O3, taken from the ICCD. Each sample was irradiated for 13 h to avoid noise when determining grain size, which was calculated using the Debye–Sherrer formula:

$$t = \frac{K\lambda}{\beta \cos\theta} \quad (1)$$

where $K=1$ was taken and $\beta=\beta_e-\beta_0$, β_e being the experimental broadening, obtained from diffraction spectra and β_0 the instrumental broadening, which has a value of 1.43×10^{-3} rad.

NiO films grown onto clear fused quartz substrates were used to obtain the optical transmission spectra. This was done with a Jasco V-630 UV-visible spectrometer, measuring from 700 to 290 nm, with air in the reference beam. The optical transmission data were taken to obtain the optical band gap considering that the NiO is a direct gap material [19].

For electrical characterization of the samples electrical contacts were painted with Electrodag 502 from Ted Pella. Results from the hot point probe showed that NiO deposited films have p-type semiconductor behavior [20]. The current–voltage characteristics for lithium-doped films were achieved with an automated system with a voltage source Keithley 230 and a picoammeter Keithley 485 both coupled to a PC.

The amount of Li incorporated in two post-deposited Li-doped NiO films grown onto alumina substrates from solutions with Li concentrations of 20% and 40% was measured by elastic recoil detection (ERD) using 12 MeV Si^{+3} ions [21]. The analysis was performed at the 3 MV Pelletron tandem accelerator at the UNAM. The Si ions impinged on sample surface at 70° respect to the surface normal, and recoiled Li atoms at 30° respect to the beam incidence were registered with a particle detector. A 7 mm Mylar filter was placed in front of the detector in order to stop scattered Si ions from the beam. These samples were also analyzed by Rutherford back scattering (RBS) using 2 MeV $^4He^{+2}$ ions to determine the concentrations of nickel and oxygen. This analysis was performed at normal incidence and the backscattered ions were registered at 167.5° respect to the beam incidence.

3. Results and discussion

Fig. 1 shows the X-ray diffraction spectra for samples deposited onto: glass substrate at 400 °C (a), fused quartz substrate at 600 °C (b) and alumina substrates at 600 °C, for a non-doped film (c) and for a 40 at% of lithium doping (d). All these spectra show well defined diffraction peaks associated with the bunsenite cubic phase of nickel oxide (00-047-1049) and which are marked with the vertical lines. The peaks associated with the cubic phase of NiO compound have practically the same location. These results might indicate that the deposited films are formed by stoichiometric nickel oxide, on all types of substrates used. Even for the samples deposited onto glass and quartz no diffraction peaks related with Ni_2O_3, $Ni(OH)_2$ and NiOOH are observed for both types of substrates. In the X-ray diffraction spectra in Fig. 1c and d, there are also diffraction peaks corresponding to the α phase of alumina substrate but no peaks related with the above mentioned nickel compounds are observed. The diffraction spectrum (Fig. 1d) for the lithium-doped sample does not show peaks associated with metallic lithium; however, the peaks obtained for deposited material show a small

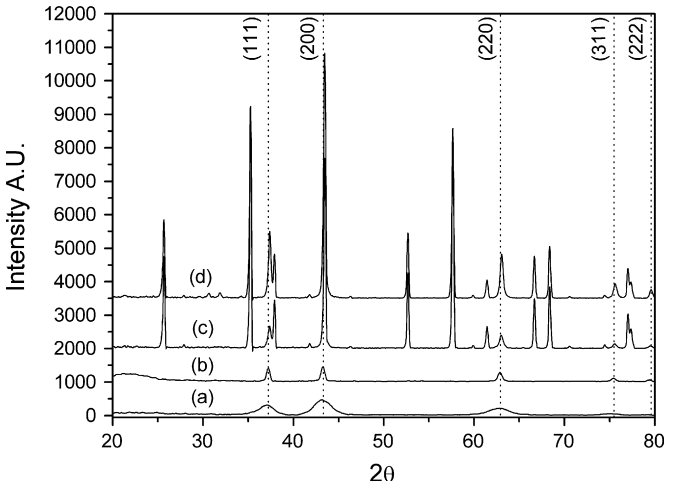

Fig. 1. X-ray diffraction spectra obtained from samples grown at 400 °C onto glass substrate (a), at 600 °C onto fused quartz substrate (b), at 600 °C onto alumina substrates without doping (c) and with a 40 at% of Li doping (d).

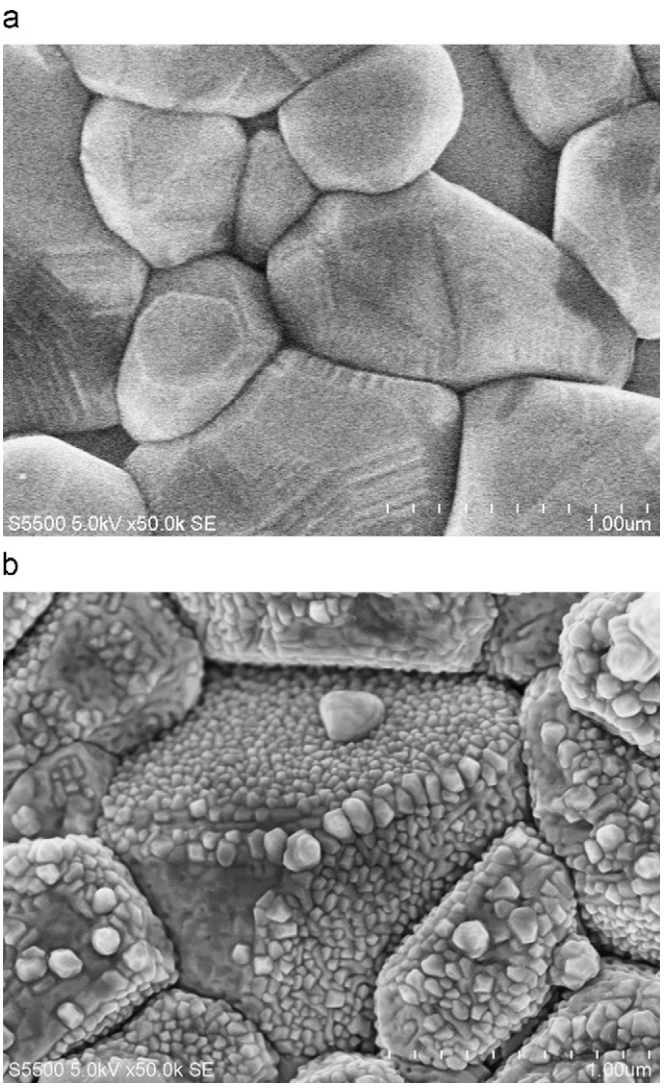

Fig. 2. HRSEM images of an alumina substrate (a) and a 40 at% lithium doped sample (b). It is to be observed that the film grows following the surface structure of the substrate.

shift toward higher values of 2Θ, which indicates that the size of the crystalline structure of the deposited material is reduced, which can be due to the formation of a lithium–nickel oxygen compound, such as: $Li_{0.208}Ni_{1.792}O_2$, $Li_{0.301}Ni_{1.699}O_2$ or $Li_{0.4}Ni_{1.6}O_2$. If the incorporation of lithium into the matrix of deposited material is in relatively higher concentration, the lattice parameters of the crystalline structure are modified and as a result the peaks are located at different values of 2Θ. Another possibility of the small shift of the diffraction peaks is the existence of internal stresses generated during the films' growth. This behavior is commonly observed in materials grown as thin films. It has been reported that as the lithium content in the films increases the shift observed in the XRD peaks is toward low values of 2Θ indicating that the doping process increased the lattice constant of the NiO crystal [22]. If there is an excess of lithium, which is not incorporated into deposited film and it does not produce any diffraction peak that can be observed in the spectrum, then that excess of lithium could be located in the grain boundaries as an amorphous phase that does not produce any X-ray diffraction peak. On the other hand, it should be cleared that although the lithium concentration in the start solution takes relatively high values during deposition by spray pyrolysis, given the high vapor pressure of Li, it is expected that not all the lithium atoms provided in the acetate molecules are incorporated in the growing film. In this deposition technique it is known that some molecules of the sprayed source materials are evaporated toward the gaseous phase due to the relatively high substrate temperature used. In the present case lithium acetate molecules must be evaporated.

The combined study by ERD and RBS confirmed that the concentration of Li incorporated in the Li-doped NiO films is lower than that provided in the start solution for film deposition. Specifically, the measured Li atomic concentrations in the films prepared from solutions with 20% and 40% of Li were $5.6 \pm 0.5\%$ and $11 \pm 0.9\%$, respectively. The results also showed an equivalent percentage reduction in the Ni content, while the O stoichiometry of the films remained almost constant, which indicates that Li atoms substitute Ni atoms in the films.

The data of the main peak (2 0 0) of the X-ray diffraction patterns were used to determine the grain size of samples grown on glass and quartz. In the case of deposition on alumina, the main peak of both oxides NiO and Al_2O_3 is located at almost the same angle: 43.276° and 43.356°, respectively; this fact does not allow to calculate the grain size using it. Then for these samples the (2 2 0) peak was used for the analysis.

The grain size obtained for the film grown onto glass substrate was 9.31 nm, which is in agreement with those reported in other works [18]. For those samples grown on quartz and alumina, without doping, the grain sizes were 93.8 and 59.4 nm, respectively. In both cases the grain sizes were bigger in comparison to that obtained from films deposited onto glass; this is expected because the grain size increases as the deposition temperature increases. In general, high substrate temperature improves crystallization and promotes the crystal growth. Even though the deposition temperature was the same for both kinds of substrates, quartz and alumina, the difference of grain sizes between deposited films may be due to the substrates' nature; while alumina is crystalline the fused quartz is amorphous, which implies different number of nucleation centers on both surfaces and therefore different crystallization rate and grain growth.

Fig. 2 shows the image of the nude surface of an alumina substrate (Fig. 2a) and an image of nickel oxide deposited at 600 °C with 40 at% lithium doping (Fig. 2b). It can be observed that the nickel oxide film grows following the topography of the substrate instead of filling the grain spaces; this can be good in

gas sensor application because the roughness is an important parameter which is related to sensitivity. On the other hand, Fig. 3 shows the dependence of the grain size of films grown onto alumina substrates as a function of lithium concentration in the spray solution. It is observed that the incorporation of lithium impurities onto the deposited material does not affect strongly the kinetics of grain growth for all the used impurity concentration. The grain size acquires values between 60 and 70 nm. This result is opposed to that reported earlier for Li-doped films deposited at room temperature by rf sputtering, where it is observed that the grain size decreases as the incorporated lithium concentration increases [22]. The slight variation in the grain size of our Li-doped films with respect to the Li content could be related to the high substrate temperature used for deposition, which favors the grain growth.

From the UV–vis optical transmission measurements carried out on the samples with different impurity concentrations, shown in Fig. 4, it is observed that the optical transmission decreases as the lithium concentration in the spray solution increases. This behavior can be due to the micro-structural features of deposited films. The thicknesses of films had values in the range from 314 to 989 nm, with the trend that the thickness increases as the lithium concentration in the start solution increases. The films deposited with low lithium concentration in the spray solution have small values for their thickness resulting in higher optical transmission. The tail observed in the optical transmission spectra in the wavelength range from 200 to 300 nm could be due to small pinholes in the deposited films such that some small fraction of light from the lamp is transmitted through the films. Meanwhile, for higher values of lithium concentration in the spray solution the deposited films show relatively low values of optical transmission for all the wavelength range studied. These samples have a textured surface without pinholes. The textured surface of these films result in a high dispersion of the incident light; this fact and the larger thickness of these films decrease the magnitude of the light transmitted through the films.

There are reports where the electronic transitions from valence band toward conduction band are analyzed as direct electronic transitions or as indirect electronic transitions. In general, the values of the optical band gap calculated considering direct allowed electronic transition or indirect electronic transition show a high dispersion in the energy range from 3.5 to 4.1 eV [23].

In the present work, the absorption coefficient values (α) were calculated from the optical transmission spectra, for all the studied samples. The calculated values of the absorption coefficient were used to obtain the optical energy band gap, considering direct electronic transitions, on the basis of the well-known relation

$$\alpha h\upsilon = A(h\upsilon - E_g)^m \quad \text{with } m = 1/2 \tag{2}$$

Fig. 5 shows the dependence of $(\alpha h\nu)^2$ as a function of the photon energy for one non-doped film and two lithium doped films (30 and 40 at% in the spray solution). In these plots the extrapolation of the linear part of the curve to its value at zero absorption coefficient determines the value of the optical band gap. The obtained values are located between 3.6 and 3.7 eV as is shown in Fig. 6. These values are consistent with those reported for crystalline nickel oxide films. This result indicates that (a) the deposited films are crystalline and (b) lithium doping of the nickel oxide films does not generate structural changes, even for the highest concentration used in the spray solution.

From the hot point probe it was determined that the conductivity type of the nickel oxide films was p-type, in all cases. The majority charge carriers where holes for both types of deposited materials, non-doped and lithium doped. This behavior can be explained if it is considered that: (a) on one hand, due to the growing process the non-doped NiO films grows with an

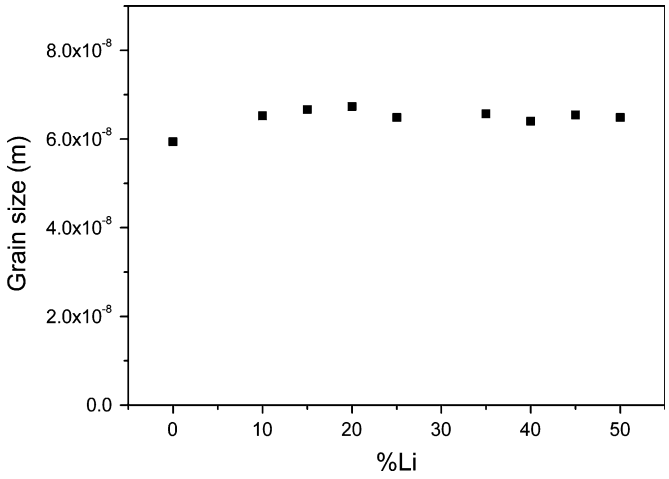

Fig. 3. Dependence of grain size as a function of lithium concentration in the start solution.

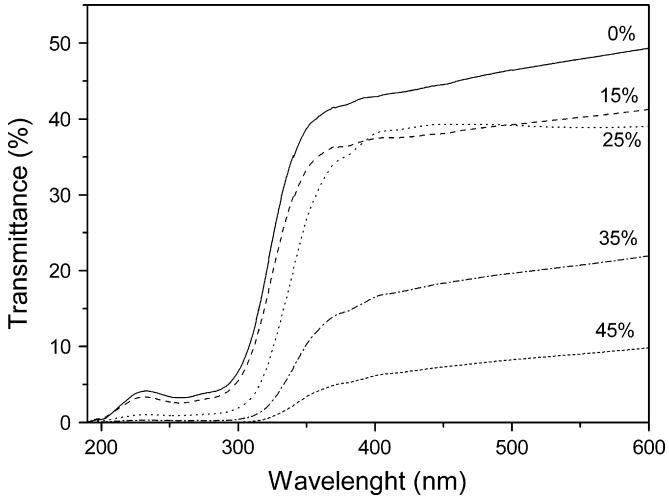

Fig. 4. Transmittance spectra of samples grown with a different concentration of Li(Ac) in the start solution.

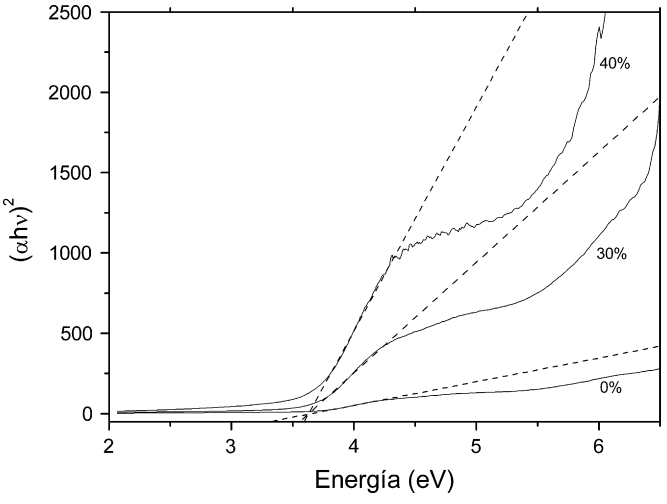

Fig. 5. Tauc plots obtained for three different samples to get the gap value.

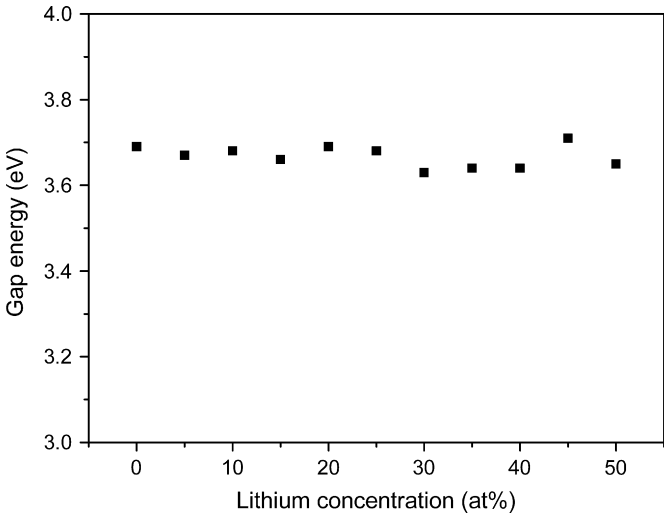

Fig. 6. Energy of the optical gap as a function of lithium concentration in the start solution.

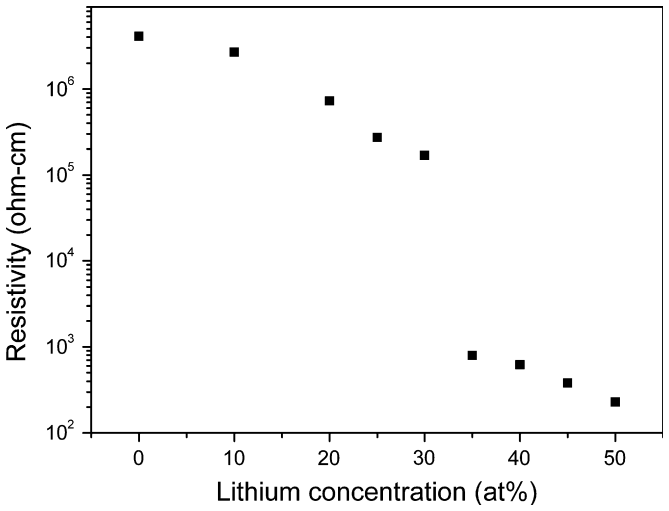

Fig. 7. Electrical resistivity as a function of lithium concentration, at ambient temperature. The descending trend of the resistivity as the concentration raises is seen, which indicates that the lithium is being incorporated as it was expected.

oxygen/nickel ratio slightly larger than one; this implies the formation of nickel vacancies in the structure, which due to their −2e charge can bind two holes that can be set free into the valence band by temperature to contribute to the conductivity. (b) On the other hand, lithium impurities are expected to replace nickel atoms in the structure and, as the lithium is added as Li^+, it can bind one hole that also can be set free by temperature to contribute to the conductivity. This could indicate that as lithium is added in the start solution the electrical conductivity of the deposited material should increase.

There are reports where the p-type electrical conductivity in non-doped films is associated with the presence of Ni^{3+}, which can be formed by Ni vacancies (V_{Ni}) in NiO, with charge balance $Ni^{2+}O^{2-}$, as is shown in the following equation:

$$V_{Ni} \rightarrow 2Ni^{3+} + 3O^{2-} \quad (3)$$

On the other hand, Ni^{3+} can be formed also by the incorporation of monovalent atoms, for instance, lithium atoms. If it is considered one molecule of nickel oxide (NiO) the addition of Li^+ can be seen as shown in the equation:

$$Li^+O^{2-} + Ni^{3+}O^{2-} \rightarrow (Li^+ + Ni^{3+})2O^{2-} \quad (4)$$

with Ni^{3+} as an acceptor center [5].

NiO films prepared by pulsed laser and by spray pyrolysis can acquire electrical conductivity n-type [24,25]. In the case of pulsed laser deposited films when oxygen is used as the working gas, if the total pressure of oxygen during deposition is low the deposited films show n-type conductivity. Meanwhile, spray deposited films with high precursor concentration in the start solution result with n-type conductivity. In NiO the vacancies occur in the cation sites, such as when the ratio O/Ni at% decreases the cation vacancies decrease and the Ni_2O_3 concentration decreases. It should be a threshold value of the O/NI ratio where no more Ni vacancies are present in the films, while the Ni_2O_3 should decrease. This trend can explain the change from p-type to n-type conductivity.

In order to analyze the electrical characteristics of non-doped films and the effect of lithium doping of nickel oxide deposited films, the current–voltage characteristics were measured. The results are shown in Fig. 7, as it can be seen, the electrical resistivity decreases as the lithium concentration increases. The electrical resistivity changes by four orders of magnitude approximately (from 10^6 to $10^2\,\Omega$ cm). It appears that there are two regions in the figure, one for lithium concentrations in the start solution up to 30 at% and the other one for higher lithium concentrations. In the first region the incorporation of lithium induces a reduction in the electrical resistivity. A similar behavior is observed in the second region since the electrical resistivity decreases as the lithium concentration increases. However, unexpectedly there is an abrupt change in the electrical resistivity for lithium concentrations between 30 and 35 at%. The doping of nickel oxide with lithium is achieved as it was explained above. But the abrupt change in the electrical resistivity could be related with the real density of nickel vacancies and the form and the number of lithium atoms being incorporated in agreement with Eq. 4. It is considered that the nickel vacancies can be singly and doubly charged vacancies [24]. In general it is suggested that the nickel vacancies are partially single and partially double charged.

4. Conclusions

Non-doped and lithium doped nickel oxide films were deposited by the pneumatic spray pyrolysis process onto quartz and onto alumina substrates. The microstructure, optical and electrical properties were analyzed. All the studied films have cubic crystalline structure related with the NiO compound. No signal related with a nickel–lithium oxygen compound was observed in the X-ray diffraction spectra. The grain size has values around 65 nm.

The optical band gap was calculated from transmission measurements, considering the allowed direct electronic transitions, obtaining values between 3.6 and 3.7 eV. The NiO deposited films show a p-type semiconductor behavior. Lithium doping reduces the electrical resistivity, from 10^6 to $10^2\,\Omega$ cm, as the lithium concentration in the start solution increases, from 0 to 50 at%. The composition analysis made for some of the Li-doped deposited films showed that only around 25% of the Li provided during film deposition is incorporated in the post-deposited films.

Acknowledgments

The authors want to thank DGAPA-UNAM for partial financial support under grant PAPIIT IN109507/20 and IN109910 and

CONACyT for scholarship support. We also want to thank L. Baños, A. Tejeda, O. Novelo and C. Flores for technical support and K. Lopez and F.J. Jaimes for accelerator operation.

References

[1] B. Sasi, K.G. Gopchandran, Nanostructured mesoporous nickel oxide thin films, Nanotechnology 18 (2007) 115613.
[2] S.W. Oh, H.J. Bang, Y.C. Bae, Y.K. Sun, Effect of calcination temperature on morphology, crystallinity, and electrochemical properties, of nano-crystalline metal oxides (Co_3O_4, CuO, and NiO) prepared via ultrasonic spray pyrolysis, J. Power Sourc. 173 (2007) 502.
[3] E. Avendaño, L. Berggren, G.A. Niklasson, C.G. Granqvist, A. Azens, Electrochromic materials and devices: brief survey and new data on optical absorption in tungsten oxide and nickel oxide films, Thin Solid Films 496 (2006) 30.
[4] H.C. Im, D.C. Choo, T.W. Kim, J.H. Kim, J.H. Seo, Y.K. Kim, Highly efficient organic light emitting-diodes fabricated utilizing nickel oxide buffer layers between the anodes and the hole transport layers, Thin Solid Films 515 (2007) 5099.
[5] P. Puspharajah, S. Radhakrishna, A.K. Arof, Transparent conducting lithium-doped nickel oxide thin films by spray pyrolysis technique, J. Mater. Sci. 32 (1997) 3001.
[6] J.A. Dirksen, K. Duval, T.A. Ring, NiO thin-film formaldehyde gas sensor, Sens. Actuat. B 80 (2001) 106.
[7] I. Hotovy, V. Rehacek, P. Siciliano, S. Capone, L. Spiess, Sensing characteristics of NiO thin films as NO_2 gas sensors, Thin Solid Films 418 (2002) 9.
[8] C. Cantalini, M. Post, D. Buso, M. Guglielmi, A. Martucci, Gas sensing properties of nanocrystalline NiO and Co_3O_4 in porous silica sol–gel films, Sens. Actuat. B 108 (2005) 184.
[9] I. Hotovy, J. Huran, J. Janík, A.P. Kobzev, Deposition and properties of nickel oxide films produced by DC reactive magnetron sputtering, Vacuum 51 (1998) 157.
[10] H.L. Chen, Y.M. Lu, W.S. Hwang, Thicknes dependence of electrical and optical properties of sputtered nickel oxide films, Thin Solid Films 514 (2006) 361.
[11] W.C. Yeh, M. Matsumura, Chemical vapor deposition of níkel oxide films from bis-π-cyclopentadienyl-nickel, Jpn. J. Appl. Phys. 36 (1997) 6884.
[12] G.E. Buono-Core, M. Tejos, G. Alveal, R.H. Hill, Níkel β-diketonate complexes as precursors for the photochemical deposition of nickel oxide thin films, J. Mater. Sci. 35 (2000) 4873.
[13] L.D. Kadam, P.S. Patil, Studies on electrochromic properties of níckel oxide thin films prepared by spray pyrolysis technique, Sol. Energy Mater. Sol. Cells 69 (2001) 361.
[14] S.A. Mahmoud, A.A. Akl, H. Kamal, K. Abdel-Hady, Opto-structural, electrical and electrochromic properties of crystalline nickel oxide thin films prepared by spray pyrolysis, Physica B 311 (2002) 366.
[15] J.D. Desai, S.K. Min, K.D. Jung, O.S. Joo, Spray pyrolytic synthesis of large area NiO_x thin films from aqueous nickel acetate solutions, Appl. Surf. Sci. 253 (2006) 1781.
[16] X. Yi, W. Wenzhong, Q. Yitai, Y. Li, C. Zhiwen, Deposition and microstructural characterization of NiO thin films by a spray pyrolysis method, J. Cryst. Growth 167 (1996) 656.
[17] M.E. Franke, T.J. Koplin, U. Simon, Metal and metal oxide nanoparticles in chemiresistors: does the nanoscale matter? Small 2 (2006) 36.
[18] B.A. Reguig, M. Regragui, M. Morsli, A. Khelil, M. Addou, J.C. Bernede, Effect of the precursor solution concentration on the NiO thin film properties deposited by spray pyrolysis, Sol. Energy Mater. Sol. Cells 90 (2006) 1381.
[19] L. Berkat, L. Cattin, A. Reguig, M. Regragui, J.C. Bernede, Comparison of the physico-chemical properties of NiO thin films deposited by chemical bath deposition and by spray pyrolysis, Mater. Chem. Phys. 89 (2005) 11.
[20] W.R. Runyan, in: Semiconductor Measurements and Instrumentation, 1st ed., McGraw-Hill, New York, 1975.
[21] J.C. Barbour, B.L. Doyle, Elastic recoil detection: ERD, in: J.R. Tesmer, M. Nastasi (Eds.), Handbook of Modern Ion Beam Materials Analysis, Material Research Society, Pennsylvania, 1995.
[22] W.L. Jang, Y.M. Lu, W.S. Hwang, W.C. Chen, Electrical properties f Li-doped NiO films, J. Eur. Ceram. Soc. 30 (2010) 503.
[23] H. Kamal, E.K. Elmaghraby, S.A. Ali, K. Abdel-Hady, Characterization of nickel oxide films deposited at different substrate temperatures using spray pyrolysis, J. Cryst. Growth 262 (2004) 424.
[24] M. Stamataki, D. Tsamakis, N. Brilis, I. Fasaki, A. Giannoudakos, M. Kompitsas, Hydrogen gas sensors based on PLD grown NiO thin films, Phys. Status Solidus A 205 (2008) 2064.
[25] B.A. Reguig, A. Khelil, L. Cattin, M. Morsli, J.C. Bernede, Properties of NiO thin films deposited by intermittent spray pyrolysis process, Appl. Surf. Sci. 253 (2007) 4330.